Influences of Induction Time and Additional LacI on the Growth Rate and Yield of the T7 Expression System in Three Escherichia Coli Strains

Nicolás Arias-Vaccari
Universidad Peruana Cayetano Heredia
Daniel Giraldez Guerra (daniel.guerra@upch.pe)
Universidad Peruana Cayetano Heredia Facultad de Ciencias y Filosofia https://orcid.org/0000-0002-2410-722X

Research Article

Keywords: Escherichia coli, IPTG, LacI, proteome allocation, T7, T7 expression system

Posted Date: January 17th, 2022

DOI: https://doi.org/10.21203/rs.3.rs-1220741/v1

Abstract

The T7 expression system is commonly used to obtain high yields of heterologous proteins in *Escherichia coli*. Still, laboratories empirically optimize its use, frequently with little information for rationally choosing the change of settings in each case. Here, we monitored the expression of green fluorescent protein (GFP) as a function of growth in three strains, with and without additional LacI repressor and IPTG added at different times. BL21(DE3) strain showed the best yield; however, its inability to repress T7 harmed the culture unless additional LacI was provided. The BLR(DE3) and MG1655 strains suppressed T7 leaking by themselves but differed in the outcomes of additional LacI. While LacI overexpression improved BLR's growth and yield, it severely harmed the MG1655 culture. In all cases, early induction with IPTG offered a better outcome than adding it too late. MG1655 was least sensitive to this timing thanks to its capability of keeping a high growth rate for longer. Notably, the GFP production rate was linear to growth rates throughout the culture, meaning that the ribosomal fraction allocated to GFP production was constant at all the analyzed time points. This observation is consistent with a general, time-resolved regulation function and supports the interpretation of our data through a proteome allocation model (PAM). A simple PAM simulated correctly the carbon overflow triggered by heterologous overexpression, indicating that if any anabolic fraction is added to compete for proteome allocation, the rate of precursors consumption will decrease, thus leading to said overflow. This model proposes that a LacI promiscuous repression activity can explain its observed opposite effects on BLR(DE3) and MG1655 strains. Through different levels of downregulation, the carbon fixating proteome fraction would reach a state closer or farther from optimum in each host.

Introduction

In the context of recombinant protein production for industrial purposes or as a reporter signal in whole-cell biosensors, expressing high amounts of a foreign gene challenges the internal cellular regulations in ways that can select non-producers or harm the culture and thereby diminish yield or signal (Binder et al., 2016; Borkowski et al., 2016; Eichmann et al., 2019; X. Jia et al., 2019; Li & Rinas, 2020; Malakar & Venkatesh, 2012). For example, the T7 promoter, induced by the IPTG-conditional derepression of T7 RNA polymerase (Browning et al., 2019; Studier & Moffatt, 1986), remains a popular system for overexpressing heterologous proteins in *Escherichia coli*(B. Jia & Jeon, n.d.; Rosano & Ceccarelli, 2014; Ting et al., 2020). Still, the protein properties, the bacterial host, and the culture conditions interact in complex ways. Therefore, it is common to follow a partially systematic set of trials to obtain an optimized protocol for protein production (Bhatwa et al., 2021).

Although BL21(DE3) has shown to be an excellent host for heterologous protein production, there is growing interest in alternative strains. For example, the relatively more versatile phenotype of K-12 strains might aid in expressing more difficult proteins or serve as a chassis for new metabolic or biosensor circuits. In particular, MG1655 is considered a laboratory wild type strain with virtually intact metabolic capabilities (Marisch et al., 2013; Wang et al., 2020). However, surprisingly few data show a simple

explicit characterization of the T7 expression system for foreign protein production as a function of culture growth in different *E. coli* strains (Kang et al., 2002).

We present here the interdependence of growth and heterologous protein production analyzed for three different *E. coli* strains under typical laboratory conditions, simultaneously monitoring culture density and GFP fluorescence. The results are interpreted through a simple kinetic system based on proteome allocation models (Scott et al., 2010; Towbin et al., 2017). In this model, a carbon-fixating proteome fraction produces intracellular precursors, while a ribosomal proteome fraction consumes these. We find that the interplay between the catabolic and anabolic proteome fractions correctly represents the effects of heterologous protein production on growth rate and carbon overflow (Li & Rinas, 2021; Weber et al., 2021). It also suggests explanatory mechanisms for the differences we observed between strains.

Materials And Methods

E. coli strains

MG1655 ΔendA ΔrecA (DE3) was a gift from Kristala Prather (Addgene code # 37854) (Tseng et al., 2010). Agar stabs of BLR(DE3) and BL21(DE3) were kindly provided by Carlos Bustamante at UC-Berkeley and Mauricio Baez at Universidad de Chile, respectively. Cells were made competent by $CaCl_2$ incubation protocol and transformed by 42°C heat shock with pUC-T7GFP or sequentially with pUC-T7GFP and pACYCDUET. Selection LB-agar plates were supplemented with 1% glucose to reduce T7 basal expression, and ampicillin for pUC-T7GFP, or ampicillin and chloramphenicol for pUC-T7GFP pACYCDUET.

Plasmids

A gene block for GFP expression was designed using Benchling RRID:SCR_013955 [Biology Software]. (2020). Retrieved from https://benchling.com. Twist Bioscience synthesized the DNA fragment. It contained the following elements: T7 promoter, lac operator, Shine-Dalgarno ribosome binding sequence, a codon-optimized GFPmut3 coding sequence (Balleza et al., 2018) fused with an LVA tag (Andersen et al., 1998) and T7 terminator. A high-copy GFP expression plasmid, pUC-T7GFP, was built by inserting this construct into a pUC57 vector through standard digestion and ligation reactions between NcoI and KpnI restriction sites. To introduce additional expression of LacI, we used the low-copy number plasmid, pACYCDUET, acquired from GenScript.

Culture protocol.

Freshly transformed colonies were hand-picked to inoculate 10 mL of medium supplemented with ampicillin or ampicillin and chloramphenicol. These cultures were incubated at 37°C and 250 RPM overnight, then measured for cell density and harvested by centrifugation at 5000 RPM for 5 minutes. Immediately, the cells were resuspended in fresh medium to the appropriate volume to obtain an optical density of 0.1, which equated to approximately $2x10^7$ cells/mL. Finally, 200 uL of these suspensions were

loaded in a 96 multiwell plate and incubated at 30°C with 220 RPM oscillatory shaking. The microcultures were grown without the addition of antibiotics. The multiwell plate was covered with its plastic lid, and the outer wells were filled with 200 uL of water so that a similar humidity surrounded all the monitored cultures. This configuration resulted in less than 2.5% volume loss due to evaporation after 16 hours. Induction was done by pipetting manually 5 uL 20 mM IPTG into the appropriate wells.

Data acquisition

Culture density (OD600) and fluorescence were monitored in a plate reader, Infinite 200 Pro from TECAN, using the following settings: 475 nm Excitation and 516 nm emission, a gain of 50, 25 flashes, reading every 15 minutes over 16 hours.

Data analysis.

Each data point averages nine measurements (three colonies in triplicate repetition). Growth rates on each point are calculated as the difference of OD between consecutive points 1 and 2, and then divided by the OD of point 1. Similarly, the production rates are calculated as the difference of fluorescence between points 1 and 2 divided by the OD at point 1. Finally, a smoothing filter was applied to the growth rate and the production rate consisting of a sliding averaging window of 5 points. Only data points until 320 minutes were used for all the analysis presented in this work.

Results

We used microcultures (200 uL) to follow the growth and heterologous protein production made by the most used strain, BL21(DE3)(Kim et al., 2017) and compared its performance with MG1655 ΔendA ΔrecA (DE3) (Tseng et al., 2010) (called MG1655 here for brevity) as representative of K12 strains, which are closest to wild type bacteria. Additionally, we monitored BLR(DE3), which is commonly the strain of choice for expressing constructs prone to spontaneous recombination. BLR(DE3) is a ΔrecA derivative of BL21(DE3) that received a ~79 Kb chromosome segment from MG1655; in consequence, it could have some traits unexpectedly different from BL21 (Goffin & Dehottay, 2017) and possibly closer to its K12 donor. We chose GFP as a generally ‘low burden’, easily folded, soluble heterologous protein to follow production in real-time through simple fluorescence measurements. The relatively fast maturing time of the GFPmut3 variant (Balleza et al., 2018) and the LVA degradation tag (Andersen et al., 1998) helped to have the best picture of the cellular activity at each time point. We used a high-copy number pUC57 vector to enhance differences in the exerted burden and their possible consequences on growth rate and protein yield. The T7 promoter, lac operator and 5’ UTR that preceded the GFP gene formed a 90 bp long sequence, identical to many public and commercial expression plasmids (e.g. pET series). Our protocol simulated the conditions most commonly used for batch protein production: diluting a pregrown culture in a rich, defined medium supplemented with glucose and amino acids. We observed the effect of additional LacI repressor expressed from its native promoter by adding a low-copy plasmid (pACYCDUET vector, with no insertion of other heterologous genes). Also, because the induction time is one of the main

variables that every laboratory needs to monitor and optimize, we compared the effects of adding IPTG at early and late time points for the six different cultures.

Cultures general behavior and yields

To produce recombinant proteins in fed-batch cultures, the induction time must correspond to a point in the growth curve when a high amount of biomass is already present (Donovan et al., 1996; Malakar & Venkatesh, 2012). Inducing too early would risk a competition that would select lower or non-producer cells due to their fitness advantage during exponential growth (Borkowski et al., 2016). Also, the induction time must ensure that the biomass-producing machinery is sustained with health and resources for long enough to achieve a good yield. The most common practice compromises an imperfect decoupling of growth from product formation by adding the inducer IPTG at OD600 of 0.5-0.7. This cell density usually corresponds to close to mid-time during exponential growth. We determined the concentration of viable bacteria in our microcultures by counting colonies from samples at six OD600 values ranging from 0.08 to 0.80. A linear regression intersecting at 0 determined an equivalence of $2x10^8$ UFC/mL per unit of OD (r^2=0.99). To evaluate the effect of the induction time, IPTG was added at a final concentration of 0.5 mM at time 0, with an OD=0.1 and 2 hours later. These two times corresponded to before and shortly after the growth-rate peak, respectively, in all cases (Figure 1). When comparing the best conditions for each strain, the growth rates and protein yields of BL21(DE3), BLR(DE3) and MG1655 were not too distant from each other (bolded text in Table 1).

On the other hand, the induction time appeared more important for BL21(DE3) and BLR(DE3) than MG1655. While the B strains lose close to 60% of their yield, MG1655 loses only ~40%. We can relate the significantly lower yield for late induction of the B strains with their sharp growth rate decrease. Differently, the growth rate of MG1655 (without pACYCDUET) decreased gentler, indicating that its anabolic activity endured longer. To test this interpretation, we introduced a reporter plasmid for GFP expression under the control of the ribosomal promoter P1. When cultured at the same conditions, we observed a peak of P1 expression centred on the growth rate peak for both MG1655 and BLR. Just as observed for the shape of their respective growth rates in time, the fluorescence of BLR strain decreased sharply, while the high values of MG1655 were kept for longer (Data not shown). Although the activities of the seven ribosomal promoters comprise a complex regulation system (Maeda et al., 2015), the extended P1 expression might be indicative of MG1655 sustaining its anabolic proteome fraction for longer times than the B strains.

Growth and Production Rates

Figure 2 shows that the protein production and growth rate are linearly related. As a foundation of the proteome allocation models, Scott et al. (2010) demonstrated a linear relationship for protein production and maximum growth rates for MG1655 cultured in different carbon sources. Here, each culture drew a straight line when the production rates at each time point were plotted against their corresponding growth rates. Table 2 indicates these linear functions for each culture. These observations support the idea that a

fixed fraction of the cell's anabolic activity is dedicated to producing the heterologous protein under the T7 expression system. However, the slopes shown in Table 2 indicate that the value of this fraction varies significantly with different hosts and their conditions of induction.

The Effect of Additional LacI

Also, we tested the influence of additional expression of LacI. While BLR and MG1655 were able to suppress the T7 expression with native LacI production solely, BL21(DE3) was severely harmed by basal expression (Figure 1A). Adding pACYCDUET plasmid, which includes the LacI gene under the control of its native promoter, increases the intracellular repressor probably by ~10 times its initial concentration. This additional LacI benefits BL21(DE3) growth during the first ~100 minutes (Figure 3A), presumably by inhibiting the early production of the foreign protein, even at the time of pre-inoculum. Intriguingly, LacI improves BLR(DE3) early growth rates, although this strain showed no detectable GFP leaking. During the first ~60 minutes, BLR benefits from additional LacI (Figure 3B), possibly by preventing an undetectable T7 leaking of GFP production, or more likely, shortening the growth lag by some other mechanism.

On the other hand, the effect of LacI was detrimental in the case of MG1655 (Figure 3C). Because this strain showed tight T7 suppression by itself, we suspect that additional LacI molecules exert their influence by repressing different promoters, i.e. other than Lac operon. High-resolution location of single molecules demonstrated that LacI binds in vivo to multiple near-specific sites (Garza de Leon et al., 2017), possibly influencing carbon fixation and anabolic activity in ways other than repressing the lac operon.

A Proteome Allocation Model

Because the initial observations seemed to fit with the concepts of proteome fractions, we felt encouraged to apply a time-resolved proteome allocation model as an attempt to represent and explain our results. We adapted the simplest model consisting of two variable proteome fractions: First, a carbon-fixating fraction, *C*, has the activity of consuming substrate from the medium and producing intracellular precursors, *x*. Second, a 'ribosomal' proteome fraction, *R*, consumes intracellular precursors to produce biomass.

The interdependence between the growth rate *m*, the intracellular precursors *x*, and the biomass-producing proteome fraction *R* is represented by the equation:

$$\mu_{(t)} = \gamma \cdot (R_{(t)} - 0.06)\left(\frac{x_{(t)}}{x_{(t)} + k_2}\right)$$

Where *g* is the absolute maximum growth rate (theoretically, for $R = 1$ and $x = \infty$) and k_2 represents the dissociation constant of *R* for its precursors (e.g., the affinity of the amino-acyl tRNA synthetases for their respective amino acids, and that of ribosomes for the amino acid-charged tRNAs). A low limit of 0.06 was set for the *R* fraction (Scott et al., 2010), representing the minimal set of anabolic reactions that the cell

needs for survival. The sum of R and C is set constant at 0.55 (Scott et al., 2010), considering the existence of a third fraction of core (Q = 0.45), constitutive genes that will not take part in the variations represented in this model.

$$R_{(t)} = 0.55 - C_{(t)}$$

The value of C is tied to the growth rate and intracellular precursors through a regulatory function:

$$\frac{dC_{(t)}}{dt} = \mu_{(t)}\left(\frac{k_f}{k_f + x_{(t)}} - C_{(t)}\right)$$

Where k_f represents the regulation sensitivity of the cell's catabolic enzymes. The value of k_f can be taken from the sensitivity of the CRP-cAMP regulatory system (Towbin et al., 2017).

To connect the intracellular precursors' production with their consumption for biomass and energy, the change of x in time is defined as:

$$\frac{dx_{(t)}}{dt} = \beta \cdot C_{(t)}\left(\frac{S_{(t)}}{S_{(t)} + k_s}\right)\left(\frac{k_1}{k_1 + x_{(t)}}\right) - \zeta\mu_{(t)}$$

Where β is the upper limit for the rate of carbon influx (theoretically, for C = 1 and S = ∞), S is the concentration of extracellular substrates, and k_s represents the dissociation constant of the C proteins for those substrates. We observed that without a feedback regulation of C activity, the precursors did not stabilize in reasonable time unless b was set to unrealistic low values. Therefore, we added a regulatory module of C activity with an allosteric constant k_1, as previously formulated by (Towbin et al., 2017). Differently than Towbin et al., we wished to represent the evolution of the precursors and extracellular substrates in time. Therefore, we added the coefficient z, representing the portion of precursors needed to sustain the growth rate m. The consumption of x (in g/litre of cell volume) towards biomass must be the rate of cell production m (in h^{-1}) multiplied by the amount of total mass per cell (cellular dry weight, $2.8 \cdot 10^{-13}$ g/cell). To obtain a realistic value for z, we took the linear dependence between glucose uptake and growth rate from a chemostat study (Carlson & Srienc, 2004) and used the data from (Scott et al., 2010), assuming that at the maximum growth rate, the carbon influx is $b \times C$ (see Supplementary Information). Additionally, using data from (Carlson & Srienc, 2004), the rate of biomass fixation was subtracted from the carbon intake to obtain the rate of x consumed towards energy production. The sources for all other constants and a complete model description are provided in the accompanying supplementary information.

Figure 4 shows a culture simulation by our PAM, when the production of a heterologous protein is induced at time 2h. Recently, it was shown that overexpressing proteins does not starve the cell of metabolic precursors but, on the opposite, causes an overflow of intermediates due to an anabolic limitation that mimics carbon overfeeding (Li & Rinas, 2021; Weber et al., 2021). In agreement with these

observations, our model shows that producing a heterologous protein causes an increase in the equilibrium concentration of intracellular precursors.

Discussion

Proteome allocation models were proposed to describe bacterial behavior at a steady state. The fact that we observe a constant slope for protein production vs growth rate suggests that the PAM general assumptions hold reasonably well through the times and cell densities analyzed here. The T7 expression system is a paradigmatic example of a high-producing circuit with a foreign regulation and a gratuitous, non-metabolizable inducer. Because of these characteristics, it is expected to interfere with cellular machinery and culture growth exclusively through the allocation of resources. However, our results suggest that its main action is not sequestering intracellular anabolic precursors but sequestering anabolic proteome fraction, in agreement with recent reports (Li & Rinas, 2021; Weber et al., 2021). As a simple, general interpretation, we propose that if any anabolic fraction is added to compete for proteome allocation, the fraction R and the rate of precursors consumption will decrease, thus leading to a carbon overflow.

Also, the expression of additional LacI appears to interfere in ways that ask for more studies and might include the repression of alternative carbon-fixating activities. In our experiments, the most striking feature of introducing additional LacI is how it affected each strain differently. Although there are many studies on LacI's structure and function regarding its allosteric mechanism and DNA binding specificity, we could not find an *in vivo* characterization of its effects on gene expression away from the lac operon. The beneficial effect of LacI in the absence of leaking (observed here for BLR(DE3)) and its harmful effect on MG1655 suggest that it may act on other sites. In *E. coli*, 14 different repressors are closely related to LacI, regulating alternative routes of carbon fixation (Fukami-Kobayashi et al., 2003). We hypothesize that, when overexpressed, LacI can downregulate carbon fixating proteins usually controlled by other transcription factors of the same family.

We attempted to represent this hypothetical action of LacI as a promiscuous transcription factor to see if its overexpression could manifest different influences depending on the cellular context. In our PAM, the repression of C fraction is a function of x with a sensitivity that relies on a constant, k_f. If k_f value is reduced 10 times, we observe that the growth rate increases, representing a beneficial effect such as that observed for BLR. If k_f is reduced 15 times, then the internal precursors x equilibrate at a lower concentration, reducing the growth rate, as in the case of MG1655. It remains to be tested if the overexpression of LacI by a low-copy number plasmid as pACYCDUET effectively represses the C fraction and if the extent of this repression is different for these strains. The model suggests that there is a level of repression of C that is optimal. It is likely that MG1655, being closer to a wild type strain, remains closer to such optimal and is therefore harmed by the overexpression of a transcription factor.

We expect that this contribution will serve as a reference to optimize heterologous protein production and to remain attentive to the rational use of LacI. BL21(DE3) remains the first choice for the highest yield

attainable, provided that additional LacI can be expressed. The capability of BLR and MG1655 to suppress uninduced expression even when using a high-copy number vector makes it unnecessary to use additional LacI repressor, which can be advantageous given the pleiotropic effects that this repressor possibly exerts on the cellular carbon metabolism. The surprisingly good yield obtained by MG1655 invites to consider its choice, especially if a high growth rate is desired for more extended periods; for instance, the development of biosensors or the insertion of new metabolic routes integrated with native carbon fluxes would benefit from the virtue of MG1655 not requiring to meddle with LacI intracellular concentration.

Finally, we encourage the application of proteome allocation models to evaluate and interpret the performance of alternative strains and conditions to maximize growth and yield.

Declarations

Statements & Declarations

Funding: This work was supported by Fondo Nacional de Desarrollo Científico, Tecnológico y de Innovación Tecnológica – FONDECYT / PROCIENCIA, through the program EF-041 - Proyectos de investigación básica y aplicada. Grant number CONV-000114-2015-FONDECYT-DE.

Competing Interests: The authors have no relevant financial or non-financial interests to disclose.

Author Contributions: Both authors contributed to the study conception and design. Nicolás Arias performed the experiments and programmed the mathematical model. Daniel Guerra provided feedback during experimental and modelling developments and wrote the first draft of the manuscript. Both authors commented on the progressing versions of the manuscript. All authors read and approved the final manuscript.

Ethics approval: This study was submitted to the projects registry of Universidad Peruana Cayetano Heredia and was considered exonerated of Ethics Committee revision.

Acknowledgments: This work was supported by **Fondo Nacional de Desarrollo Científico, Tecnológico y de Innovación Tecnológica – FONDECYT / PROCIENCIA**, through the program **EF-041 - Proyectos de investigación básica y aplicada**. Grant number **CONV-000114-2015-FONDECYT-DE**.

References

Andersen, J. B., Sternberg, C., Poulsen, L. K., Bjørn, S. P., Givskov, M., & Molin, S. (1998). New Unstable Variants of Green Fluorescent Protein for Studies of Transient Gene Expression in Bacteria. *Applied and Environmental Microbiology*, *64*(6), 2240–2246.

Balleza, E., Kim, J. M., & Cluzel, P. (2018). Systematic characterization of maturation time of fluorescent proteins in living cells. *Nature Methods*, *15*(1), 47–51. https://doi.org/10.1038/nmeth.4509

Bhatwa, A., Wang, W., Hassan, Y. I., Abraham, N., Li, X.-Z., & Zhou, T. (2021). Challenges Associated With the Formation of Recombinant Protein Inclusion Bodies in Escherichia coli and Strategies to Address Them for Industrial Applications. *Frontiers in Bioengineering and Biotechnology*, *9*, 630551. https://doi.org/10.3389/fbioe.2021.630551

Binder, D., Probst, C., Grünberger, A., Hilgers, F., Loeschcke, A., Jaeger, K.-E., Kohlheyer, D., & Drepper, T. (2016). Comparative Single-Cell Analysis of Different E. coli Expression Systems during Microfluidic Cultivation. *PLoS ONE*, *11*(8), e0160711. https://doi.org/10.1371/journal.pone.0160711

Borkowski, O., Ceroni, F., Stan, G.-B., & Ellis, T. (2016). Overloaded and stressed: Whole-cell considerations for bacterial synthetic biology. *Current Opinion in Microbiology*, *33*, 123–130. https://doi.org/10.1016/j.mib.2016.07.009

Browning, D. F., Godfrey, R. E., Richards, K. L., Robinson, C., & Busby, S. J. W. (2019). Exploitation of the Escherichia coli lac operon promoter for controlled recombinant protein production. *Biochemical Society Transactions*, *47*(2), 755–763. https://doi.org/10.1042/BST20190059

Carlson, R., & Srienc, F. (2004). Fundamental Escherichia coli biochemical pathways for biomass and energy production: Creation of overall flux states. *Biotechnology and Bioengineering*, *86*(2), 149–162. https://doi.org/10.1002/bit.20044

Donovan, R. S., Robinson, C. W., & Glick, B. R. (1996). Review: Optimizing inducer and culture conditions for expression of foreign proteins under the control of the lac promoter. *Journal of Industrial Microbiology*, *16*(3), 145–154. https://doi.org/10.1007/BF01569997

Eichmann, J., Oberpaul, M., Weidner, T., Gerlach, D., & Czermak, P. (2019). Selection of High Producers From Combinatorial Libraries for the Production of Recombinant Proteins in Escherichia coli and Vibrio natriegens. *Frontiers in Bioengineering and Biotechnology*, *7*, 254. https://doi.org/10.3389/fbioe.2019.00254

Fukami-Kobayashi, K., Tateno, Y., & Nishikawa, K. (2003). Parallel evolution of ligand specificity between LacI/GalR family repressors and periplasmic sugar-binding proteins. *Molecular Biology and Evolution*, *20*(2), 267–277. https://doi.org/10.1093/molbev/msg038

Garza de Leon, F., Sellars, L., Stracy, M., Busby, S. J. W., & Kapanidis, A. N. (2017). Tracking Low-Copy Transcription Factors in Living Bacteria: The Case of the lac Repressor. *Biophysical Journal*, *112*(7), 1316–1327. https://doi.org/10.1016/j.bpj.2017.02.028

Goffin, P., & Dehottay, P. (2017). Complete Genome Sequence of Escherichia coli BLR(DE3), a recA-Deficient Derivative of E. coli BL21(DE3). *Genome Announcements*, *5*(22), e00441-17. https://doi.org/10.1128/genomeA.00441-17

Jia, B., & Jeon, C. O. (n.d.). High-throughput recombinant protein expression in Escherichia coli: Current status and future perspectives. *Open Biology*, *6*(8), 160196. https://doi.org/10.1098/rsob.160196

Jia, X., Bu, R., Zhao, T., & Wu, K. (2019). Sensitive and Specific Whole-Cell Biosensor for Arsenic Detection. *Applied and Environmental Microbiology*, *85*(11), e00694-19. https://doi.org/10.1128/AEM.00694-19

Kang, D. G., Kim, Y. K., & Cha, H. J. (2002). Comparison of green fluorescent protein expression in two industrial Escherichia coli strains, BL21 and W3110, under co-expression of bacterial hemoglobin. *Applied Microbiology and Biotechnology*, *59*(4–5), 523–528. https://doi.org/10.1007/s00253-002-1043-3

Kim, S., Jeong, H., Kim, E.-Y., Kim, J. F., Lee, S. Y., & Yoon, S. H. (2017). Genomic and transcriptomic landscape of Escherichia coli BL21(DE3). *Nucleic Acids Research*, *45*(9), 5285–5293. https://doi.org/10.1093/nar/gkx228

Li, Z., & Rinas, U. (2020). Recombinant protein production associated growth inhibition results mainly from transcription and not from translation. *Microbial Cell Factories*, *19*(1), 83. https://doi.org/10.1186/s12934-020-01343-y

Li, Z., & Rinas, U. (2021). Recombinant protein production-associated metabolic burden reflects anabolic constraints and reveals similarities to a carbon overfeeding response. *Biotechnology and Bioengineering*, *118*(1), 94–105. https://doi.org/10.1002/bit.27553

Maeda, M., Shimada, T., & Ishihama, A. (2015). Strength and Regulation of Seven rRNA Promoters in Escherichia coli. *PLOS ONE*, *10*(12), e0144697. https://doi.org/10.1371/journal.pone.0144697

Malakar, P., & Venkatesh, K. V. (2012). Effect of substrate and IPTG concentrations on the burden to growth of Escherichia coli on glycerol due to the expression of Lac proteins. *Applied Microbiology and Biotechnology*, *93*(6), 2543–2549. https://doi.org/10.1007/s00253-011-3642-3

Marisch, K., Bayer, K., Scharl, T., Mairhofer, J., Krempl, P. M., Hummel, K., Razzazi-Fazeli, E., & Striedner, G. (2013). A comparative analysis of industrial Escherichia coli K-12 and B strains in high-glucose batch cultivations on process-, transcriptome- and proteome level. *PloS One*, *8*(8), e70516. https://doi.org/10.1371/journal.pone.0070516

Rosano, G. L., & Ceccarelli, E. A. (2014). Recombinant protein expression in Escherichia coli: Advances and challenges. *Frontiers in Microbiology*, *5*, 172. https://doi.org/10.3389/fmicb.2014.00172

Scott, M., Gunderson, C. W., Mateescu, E. M., Zhang, Z., & Hwa, T. (2010). Interdependence of cell growth and gene expression: Origins and consequences. *Science (New York, N.Y.)*, *330*(6007), 1099–1102. https://doi.org/10.1126/science.1192588

Studier, F. W., & Moffatt, B. A. (1986). Use of bacteriophage T7 RNA polymerase to direct selective high-level expression of cloned genes. *Journal of Molecular Biology*, *189*(1), 113–130. https://doi.org/10.1016/0022-2836(86)90385-2

Ting, W.-W., Tan, S.-I., & Ng, I. (2020). Development of chromosome-based T7 RNA polymerase and orthogonal T7 promoter circuit in Escherichia coli W3110 as a cell factory. *Bioresources and Bioprocessing*. https://doi.org/10.1186/s40643-020-00342-6

Towbin, B. D., Korem, Y., Bren, A., Doron, S., Sorek, R., & Alon, U. (2017). Optimality and sub-optimality in a bacterial growth law. *Nature Communications*, *8*, 14123. https://doi.org/10.1038/ncomms14123

Tseng, H.-C., Harwell, C. L., Martin, C. H., & Prather, K. L. J. (2010). Biosynthesis of chiral 3-hydroxyvalerate from single propionate-unrelated carbon sources in metabolically engineered E. coli. *Microbial Cell Factories*, *9*, 96. https://doi.org/10.1186/1475-2859-9-96

Wang, J., Huang, C., Guo, K., Ma, L., Meng, X., Wang, N., & Huo, Y.-X. (2020). Converting Escherichia coli MG1655 into a chemical overproducer through inactivating defense system against exogenous DNA. *Synthetic and Systems Biotechnology*, *5*(4), 333–342. https://doi.org/10.1016/j.synbio.2020.10.005

Weber, J., Li, Z., & Rinas, U. (2021). Recombinant protein production provoked accumulation of ATP, fructose-1,6-bisphosphate and pyruvate in E. coli K12 strain TG1. *Microbial Cell Factories*, *20*(1), 169. https://doi.org/10.1186/s12934-021-01661-9

Tables

Table 1.

	Plasmids					
	pUC-T7GFP			pUC-T7GFP + pACYCDUET		
	No induction	$IPTG_{0H}$	$IPTG_{2H}$	No induction	$IPTG_{0H}$	$IPTG_{2H}$
Strains	Maximum Fluorescence/OD					
BL21	8103 ± 1271	8289 ± 6455	6763 ± 5271	196 ± 3	**8423** ± 317	3548 ± 624
BLR	375 ± 9.5	3934 ± 113	2013 ± 123.5	350 ± 5	**7509** ± 1335	2847 ± 681
MG1655	143 ± 13	**5601** ± 237	3252 ± 115	205 ± 5	1815 ± 301	652 ± 105

Table 2.

	Plasmids			
	pUC-T7GFP		pUC-T7GFP + pACYCDUET	
Strain	$IPTG_{0H}$	$IPTG_{2H}$	$IPTG_{0H}$	$IPTG_{2H}$
BL21(DE3)	7014.0*μ +385.4	8884.5*μ -314.7	8089.2*μ +698.6	5335.7*μ +381.8
BLR(DE3)	4503.57*μ -80.69	4637.13*μ -351.03	4297.9*μ +753.1	3362.97*μ +349.15
MG1655	5709.3*μ +248.4	2864.5*μ +539.7	3217.05*μ -95.76	1591.72*μ -26.93

Figures

Figure 1

Growth and GFP production rates. Microcultures (200 uL) started at OD600 = 0.1 (~2⁰10^7 UFC/mL) and were induced with 0.5 mM IPTG as indicated. ***Left panels***, cells transformed with pUC-T7GFP. ***Right panels***, cells transformed with pUC-T7GFP and pACYCDUET for additional expression of LacI. **A**, BL21(DE3). **B**, BLR(DE3). **C**, MG1655.

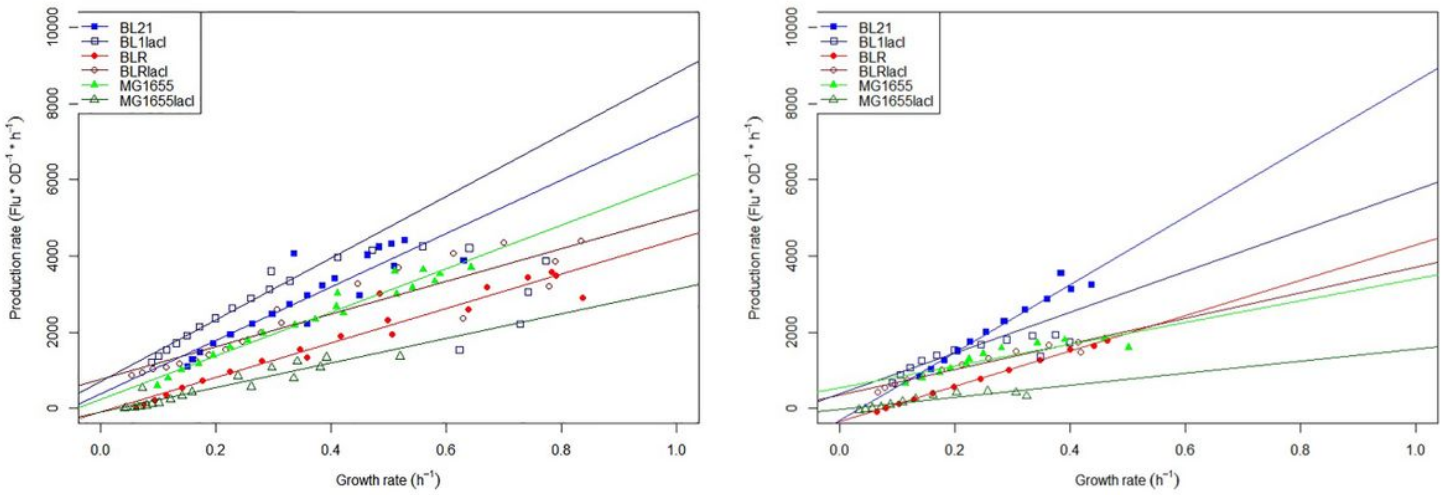

Figure 2

Protein production rates as a function of growth rates. **A**, cultures were induced with 0.5 mM IPTG at the start point. **B**, cultures were induced with 0.5 mM IPTG at time = 2h. Plotted data correspond to the first 320 minutes to avoid including the onset of the stationary phase.

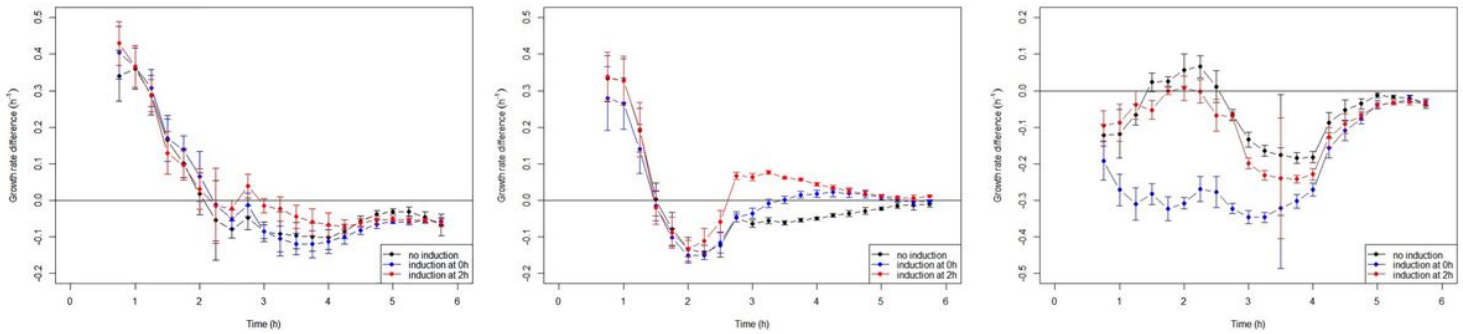

Figure 3

Effect of LacI on growth rates. At each time point, the change in the growth rate of cells transformed with both pUC-T7GFP and pACYCDUET was calculated by subtraction, taking as a reference the non-induced strain transformed only with pUC-T7GFP. Positive values indicate a beneficial effect of the additional LacI expression induced by pACYCDUET. **A**, BL21(DE3). **B**, BLR(DE3). **C**, MG1655.

Figure 4

Simulation of cultures by a time-resolved PAM. ***Left panels***, simulations with no heterologous protein. ***Right panels***, simulations of cultures induced for the production of a heterologous at time = 2 h, indicated by the vertical line. **A,** Concentration of the extracellular substrates S, and intracellular precursors x. **B,** Growth rate, rate of heterologous protein production, and total number of cells. **C**, Proteome fractions allocated by: *C*, carbon-fixating proteins, *R*, anabolic or ribosomal proteins, and *H*, heterologous protein.

Supplementary Files

This is a list of supplementary files associated with this preprint. Click to download.

- 152912911274Authorchecklist.pdf
- InfluencesofSUPPINFO.docx
- InfluencesofRawDataFluorescence.xlsx
- InfluencesofRawDataOD600.xlsx